

## Synthesis of Carbon Quantum Dots from Rice Straw Using the Hydrothermal Method

Duy-Hoang Nguyen<sup>1</sup>, Son Van Nguyen<sup>2</sup>, Trieu Khoa Nguyen<sup>1,\*</sup>

Received 12/9/2024  
Accepted 2/23/2025

DOI: 10.22034/ijnn.2025.2047781.2610

International Journal of Nanoscience and  
Nanotechnology

### Abstract

As a form of nanomaterial, Carbon Dots (CDs) attracted the attention of researchers due to their diverse raw material sources, low cost, ease of preparation, and numerous applications in optics, biomedicine, and energy. Our research article focused on the production of Carbon Quantum Dots (CQDs) derived from rice straw using a bottom-up approach. As the next steps, UVA lamps, SEM, FTIR, UV-Vis, and PL were used as the main analysis techniques for the aqueous solution of CDs, as well as dried CDs. Under UV light, the color of the aqueous solution of CDs changed from yellow-brown to green, indicating that CDs had formed. Subsequent SEM images showed that the average particle size of the CDs was 20 nm. Besides, FTIR analysis illustrated functional groups such as O-H, C-H, C=O, N-H, C-OH, and C-O of CQDs. Furthermore, the UV-Vis spectrum indicated suitable optical properties for pollutant interaction, while the PL spectrum confirmed strong fluorescence with excitation-dependent behavior, making these CQDs excellent candidates for sensing applications. Thus, the analytical results showed that the synthesized CQDs had suitable properties for wastewater treatment applications. Hence, this study highlighted the feasibility of converting agricultural waste into functional nanomaterials, contributing to sustainable nanotechnology and environmental management.

**Keywords:** Rice Straw, Carbon Quantum Dots (CQDs), Fourier-transform Infrared Spectroscopy (FTIR), Ultraviolet-visible (UV-Vis) Spectrum, Photoluminescence (PL)

### How to cite this article

Nguyen DH, Nguyen SV, Nguyen TK. Synthesis of Carbon Quantum Dots from Rice Straw Using the Hydrothermal Method. *Int. J. Nanosci. Nanotechnol.*, 2025;1: 31-39. DOI: 10.22034/ijnn.2025.2047781.2610

### 1. Introduction

Micro and nanofabrication techniques are increasingly becoming a popular research trend among scientists worldwide, in which the synthesis of carbon dots (CDs) nanomaterials has attracted significant interest and appreciation for their specialized applications. They were first discovered in 2004 during the manipulation of single-wall carbon nanotubes, and they share a similar structure. These materials consist of sp<sup>2</sup>/sp<sup>3</sup> hybrid carbon networks with functional groups such as carboxylic acid, hydroxyl, carboxyl, amino, and epoxy, enabling them to readily bond with inorganic and organic radicals [1]. Although CDs are only a few nanometers in size, they are easy to prepare, inexpensive, and possess outstanding features such as chemical sensors, food safety, photocatalysis, and particularly in medicine due to the low toxicity of CDs [1, 2].

CDs can be classified into three main types [2, 4, 5], including graphene quantum dots (GQDs), polymer dots

(PDs), and carbon nanodots (CNDs). Spherical carbon nanodots (CNDs) can be classified into two subgroups: Carbon nanoparticles (CNPs) and carbon quantum dots (CQDs). CNPs are amorphous with no clear crystal lattice and don't exhibit quantum confinement effects (QCE). In contrast, CQDs consist of multiple graphene layers and surface chemical groups, enabling them to exhibit QCE. There are two main approaches to preparing CDs, as proposed by Biswajit Gayen et al. [1] and Saheed E. Elugoke et al. [4]: the top-down approach and the bottom-up approach, depending on the substrate and the reaction method. The top-down approach includes the arc-discharge method, electrochemical oxidation method, chemical oxidation method, laser ablation method, and ultrasonication method [1, 4]. However, these methods are not very popular due to their high material and machinery requirements. On the other hand, the bottom-up approach, such as the hydrothermal method, solvothermal method, carbonization method, microwave method, and pyrolysis method [1, 4], is more popular because it is cost-effective and easy to implement. In particular, the hydrothermal method is widely used for preparing CDs [6].

One of the reasons that the hydrothermal method

<sup>1</sup> Faculty of Mechanical Engineering, Industrial University of Ho Chi Minh, Ho Chi Minh City, Vietnam.

<sup>2</sup> Advanced Technology Center - Le Quy Don Technical University, Vietnam.

E-mail: [nguyenkhoatrieu@iuh.edu.vn](mailto:nguyenkhoatrieu@iuh.edu.vn)



is so popular, in addition to the simple process and inexpensive equipment, is that this method can also synthesize CDs from agricultural waste. Nowadays, the agricultural industry wastes a significant amount of green raw materials every day, leading to a loss of resources, money, and social labor. As a solution, there have been many research works aimed at producing CDs from these green materials. CDs can be synthesized from various sources such as watermelon peel [7], gromwell's roots [8], walnut shells [9], sucrose [10], glucose [11], wine cork [12], citric acid, and L-histidine [13]. Additionally, CDs have also been synthesized from rice straw using the hydrothermal method [14-16]. Furthermore, CDs could also be synthesized from *Chionanthus retusus* (*C. retusus*) fruit extract using a simple hydrothermal-carbonization method [17]. From these research works, it became evident that the parameters of temperature, water amount, and volume needed to be adjusted based on the input material. Therefore, determining suitable process parameters to synthesize CDs to create more added value for agricultural waste products, such as rice straw, is an urgent need.

In recent years, agricultural waste has emerged as a promising precursor for the development of carbon-based nanostructures for environmental applications, particularly in wastewater purification. Various studies have demonstrated the potential of biomass-derived carbon materials, including activated carbon, porous carbon, and aerogel-based nanostructures, for removing contaminants such as heavy metals, organic pollutants, and dyes. For instance, highly porous activated carbon materials obtained from carbonized biomass have shown significant CO<sub>2</sub> capture capacity and adsorption properties [18]. Similarly, novel carbon nanostructures, carbon nanotubes (CNTs), synthesized from agricultural residues have been explored for catalytic and adsorption-based water treatment, highlighting the sustainable conversion of waste into functional materials [19]. Recent research has further expanded this approach by utilizing pulping by-products to produce aerogel-based carbon nanostructures for enhanced dye adsorption, thereby addressing industrial wastewater contamination [20]. Additionally, activated porous carbon derived from rice straw residues with potassium ferrate-assisted activation has exhibited remarkable efficiency in cationic and anionic dye adsorption, demonstrating the versatility of biomass-based carbon materials [21]. Advanced aerogel-carbon nanostructures have also been developed from rice straw - pulping black liquors, further enhancing adsorption capacity for various pollutants [22]. Furthermore, the regulation of pore size in activated carbon catalysts has significantly improved their performance in catalytic ozonation, a process used for advanced water treatment [23]. While these studies highlight the adsorption-driven mechanisms of traditional carbon nanostructures, CQDs synthesized from agricultural waste such as rice straw present a unique multifunctional approach to wastewater purification. Unlike conventional activated carbon or porous carbon materials, CQDs exhibit fluorescent properties, allowing for real-time pollutant detection alongside adsorption-based removal. Moreover, their

surface functionalization with oxygen-containing groups enhances their interactions with pollutants, offering a potential advantage in selective adsorption and sensing applications. Given these distinctive features, the present study aims to explore the synthesis and characterization of CQDs from rice straw, emphasizing their potential role in sustainable wastewater treatment compared to existing biomass-derived carbon nanomaterials.

This research focused on the extraction of CQDs from rice straw utilizing a minimalist and straightforward procedure. The methodology was designed to be easily executable without the need for additional chemical catalysts while ensuring the production of CQDs at the nanoscale. Using pre-cleaned rice straw, CQDs were synthesized via a hydrothermal method, and the coarse residue was subsequently removed from the mixture by centrifugation. In the next step, the CQDs were filtered through a membrane filter with a pore diameter of 0.22 μm. The following steps involved the use of UVA lamps, SEM, and FTIR as the primary analysis techniques for both the aqueous solution of CDs and dried CDs. Under UV light, the aqueous solution of CDs changed color from yellow-brown to green, indicating the formation of CDs. SEM images revealed that the average particle size of the CDs was about 20 nm. Additionally, FTIR analysis identified functional groups such as O-H, C-H, C=O, N-H, C-OH, and C-O in the CDs. Furthermore, the UV-Vis spectrum indicated suitable optical properties for pollutant interaction, while the PL spectrum confirmed strong fluorescence with excitation-dependent behavior, making these CQDs excellent candidates for sensing applications.

The novelty of our work lies in the first work on the synthesis and characterization of CQDs from Vietnamese rice straw, as a widely available agricultural waste. The obtained CQD possesses many advantages for wastewater treatment, such as low toxicity, easy synthesis and functionalization, high water solubility, rich functional groups (O-H, C=O, C-OH), fluorescence properties, and photocatalytic properties, which enhance their adsorption efficiency, sensing ability, and pollutant degradation. The performance of CQDs in wastewater treatment is superior to traditional materials such as activated carbon and carbon nanotubes. Unlike activated carbon and carbon nanotube, which primarily rely on adsorption, CQD offers more versatile treatment options, including adsorption, photocatalytic, and sensing capacity. Furthermore, CQDs have lower toxicity, are easier to synthesize, and have higher water solubility than activated carbon and carbon nanotube, which are advantageous in wastewater treatment.

## 2. Materials and Methods

### 2.1. Materials

Rice straw was collected from a local rice paddy field in Vietnam. For hydrothermal applications, Hanna HI70436 deionized water was utilized. The filtration step involved employing a PTFE sterilized syringe filter head with a 33 mm diameter and 0.22 μm filter pore size from Finetech. A KH35A Drying oven (KENTON) with an inner size of

350×350×350 mm<sup>3</sup>, a temperature accuracy of ±1 °C, and a capacity of 43L was employed. Centrifugation was carried out using a DLAB SCIENTIFIC DM0506 centrifuge operating at 300 - 5000 rpm.

### 2.2. Synthesis of CDs

Starting with 0.2 g of rice straw, it underwent a thorough cleansing involving immersion in 99.5% alcohol followed by thorough drying. The dried straw was then cut into small pieces and introduced into a Teflon-coated hydrothermal autoclave. The small rice straw was accompanied by precisely 15 milliliters of deionized water. As the next step, the autoclave was placed in the oven. Subsequently, the mixture was sealed in a 50 mL Teflon-lined stainless-steel autoclave, heated at 220 °C for 12 hours, and cooled to room temperature naturally. Upon procedure, the resulting mixture underwent centrifugation at 5000 rpm for 30 minutes to separate the insoluble residue of the CDs aqueous solution mixture. Following the step, a Syringe Filter with a pore size of 0.22 μm was employed to procure the CDs aqueous solution. Finally, the Carbon Dots aqueous solution is stored in a cool environment to ensure optimal conditions for subsequent processes. This procedure is illustrated in Figure 1.

### 2.3. Characterization of CDs

A DS-6W UVA bulb with a wavelength range of 350-375 nm, manufactured by Philips, was used for the initial observation of the sample after synthesis. HITACHI SEM-S4800 with voltage 10 kV and 180k magnification was used to observe the morphology and measure the size of CDs. As the next step, the Fourier transform infrared (FT-IR) spectrum was obtained using an ATR-IR, Cary 630 Agilent spectrophotometer.

The optical properties of the obtained CQDs were determined using a Hitachi double-beam spectrophotometer (UV-Vis/NIR, FL) UH5300. For the sake of reproducibility, the parameters for the UV-Vis

measurement are presented in Table 1.

In the next step of optical properties analysis, a detailed photoluminescence (PL) study was performed using an Agilent CaryEclipse fluorescence spectrophotometer with the parameters listed in Table 2.

**Table 1.** Instrument parameters for UV-Vis measurement.

Instrument parameters	Setting	Unit
Measurement Mode	WL Scan	-
Data Mode	Abs	-
Start WL	1000.0	nm
End WL	200.0	nm
Scan Speed	400	nm/min
Data Interval	2.0	nm
Initial Delay	0	s
Bandpass	1.0	nm
Response	Medium	-
6 Cell Mode	Manual	-

**Table 2.** Instrument parameters for PL measurements.

Instrument parameters	Setting	Unit
Data mode	Fluorescence	-
Scan mode	Emission	-
X Mode	Wavelength	nm
Start	300-700	nm
End WL	800	nm
Ex. Wavelength	280-700	nm
Ex. Slit	10	nm
Em. Slit	10	nm
Scan rate	600	nm/min
Data Interval	1.0	nm
Averaging Time	0.1	s
Excitation filter	Auto	-
Emission filter	360 - 1100	nm
PMT voltage	Medium	V
Corrected spectra	OFF	-
Smoothing	ON	-
Type	Savitzky-Golay	-

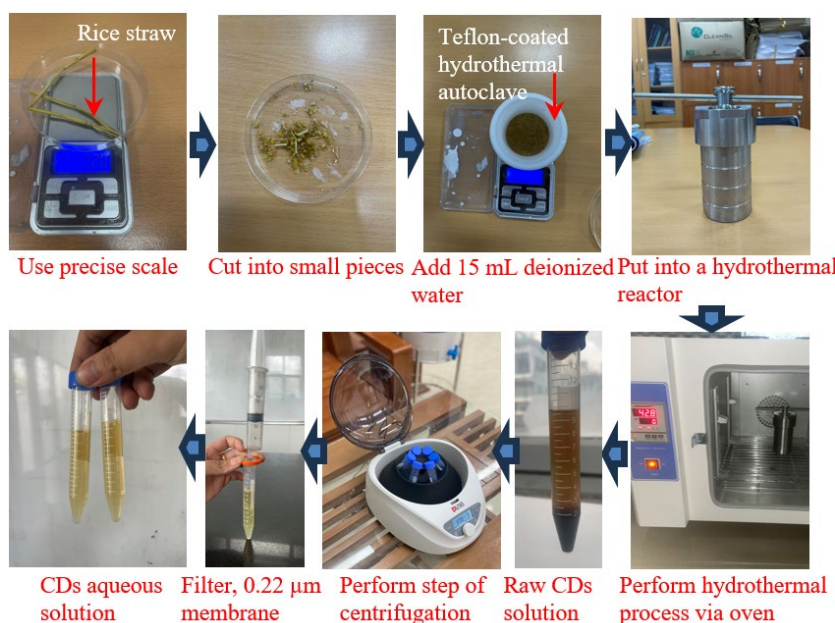


**Figure 1.** The synthesis procedure of CDs.

### 3. Results and Discussion

#### 3.1. Observation under UV light

Numerous studies have shown a remarkable tendency for CDs to change color under ultraviolet light [8, 14]. This is a characteristic attributed to the sensitivity of the optical absorption and luminescence features of CDs [1, 3, 8, 14]. Photoluminescence studies have demonstrated that the light emission and color of CDs depend on factors such as their size, pH, original material source, surface functionalization, thermal conditions [4, 8], and excitation wavelength [2]. Therefore, using UV light to illuminate a solution of carbon dots serves as a reliable method for confirming the successful synthesis of CDs [8]. The samples included the aqueous solution of CDs and deionized water, both exposed to UVA illumination within the wavelength range of 350-375 nm. The aqueous solutions of CDs showed a color change from yellow-brown to green, as shown in Figure 2, indicating that CDs were formed. This fascinating phenomenon highlights the complex interaction between the functional groups and chemical properties of CDs. This sheds light on their potential for diverse applications in optoelectronic devices, sensor platforms, and filtration applications. On the right side, under UV light with wavelengths ranging from 350 to 375 nm, the CDs aqueous solution changed color from yellow-brown to green, whereas the deionized water remained unchanged.

#### 3.2. Morphology and dimension of CDs

After completing the filtration process, the CDs aqueous solution was meticulously deposited on the foil base with a few drops. This aqueous solution-filled substrate underwent heating at 70 °C for 10 minutes, followed by a controlled temperature decrease to 50 °C over 10 minutes. Subsequently, this sample underwent analysis via SEM to evaluate the dimensions of the CDs.

The SEM analysis unveiled that the dried CDs exhibit a size spectrum ranging from 15.6 to 24.2 nm, and the average particle size of the CDs was about 20 nm, as shown in Figure 3. While the sizes of the dried CDs are slightly larger than those reported in previous studies, as listed in Table 3, they still affirm the efficacy of the straw-based synthesis method in yielding nano-sized particles.

The particle size reported in the current study is based on scanning electron microscopy (SEM) analysis, which measures dried samples and may show larger sizes due to aggregation effects. Aggregation effects in SEM measurements refer to the tendency of nanoparticles to cluster or agglomerate when dried onto a substrate for imaging [24]. This can lead to an overestimation of the individual particle size for several reasons [25]. SEM samples are typically prepared by drop-casting a nanoparticle suspension onto a solid substrate (such as silicon or a conductive carbon tape) and allowing it to dry. As the solvent evaporates, nanoparticles may

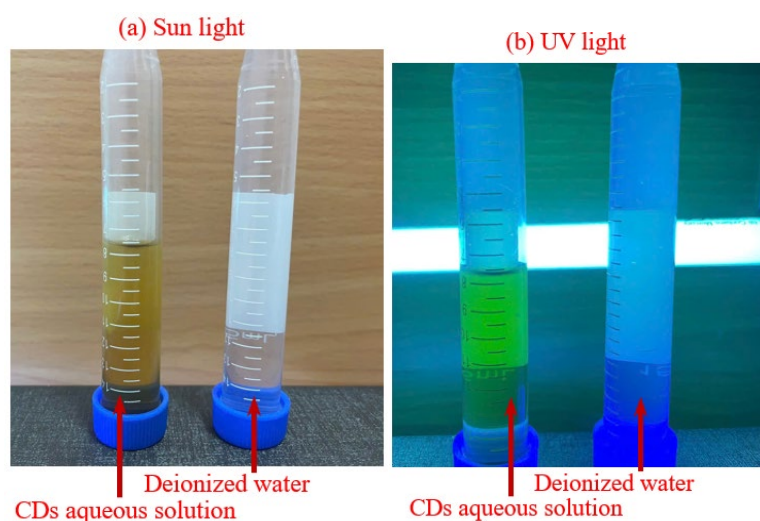


**Figure 2.** (a) The aqueous solution of CDs on the left and deionized water on the right under sunlight. (b) The aqueous solution of CDs on the left and deionized water on the right under UVA illumination with wavelengths ranging from 350-375 nm.

**Table 3.** Sizes of CDs extracted from various components in referenced literature.

Synthesis method	Precursor	Size	Reference
Hydrothermal	Gromwell	9.1 nm	[8]
Carbonization combined with chemical	Walnut shells	1 - 10 nm (Average = 3.4 nm)	[9]
Hydrothermal	Sucrose	8 - 9 nm	[10]
Hydrothermal	Waster wine cork	3.5-8.9 nm	[12]
Hydrothermal	Citric acid and L-histidine	3.9 nm	[13]
Hydrothermal	Wheat straw	Average 2.1 nm	[14]
Hydrothermal	Rice Straw mixed with H <sub>3</sub> PO <sub>4</sub> and ultrasonicated	8 nm - 11 nm (Average = 9 nm)	[15]
Hydrothermal	Rice straw	~45 nm	[16]
Hydrothermal	Chionanthus retusus fruit	3 nm ~ 7 nm	[17]

come closer together due to capillary forces, causing them to form larger aggregates rather than remaining as isolated particles. The second reason may be due to surface interaction effects. Nanoparticles may interact with the substrate surface through van der Waals forces, electrostatic interactions, or hydrogen bonding. This can cause them to cluster in an irregular manner, affecting the measurement of individual particle size. Third, in some cases, the high-energy electron beam of the SEM itself can induce charging effects on non-conductive samples, leading to particle movement or further aggregation. Finally, since SEM provides only surface imaging (without penetration into the sample), it does not differentiate between overlapping or stacked nanoparticles, making it appear as though the particles are larger than they actually are. Due to these aggregation effects, the observed particle size in SEM images may be significantly larger than the actual size of individual nanoparticles in solution. To obtain a more accurate size measurement, High-Resolution Transmission Electron Microscopy (HR-TEM), Atomic Force Microscopy (AFM), or Dynamic Light Scattering (DLS) are often used, as these techniques allow for better particle dispersion and solution-phase analysis [25].

### 3.3. Fourier transform infrared (FT-IR) spectrum of CDs

The FT-IR spectrum analysis of CDs after drying the aqueous CDs solution revealed the presence of functional groups. The spectrum began with a strong peak at  $3275\text{ cm}^{-1}$ , corresponding to the stretching vibration of O-H bonds [26-28]. Additionally, peaks at  $2913\text{ cm}^{-1}$  and  $825\text{ cm}^{-1}$  indicated the stretching vibration and deformation vibration of C-H bonds [26-28], respectively. A peak at  $1645\text{ cm}^{-1}$  indicated the presence of C=O bonds [26-28]. A deformation band of N-H bonds [26, 27] was observed at  $1562\text{ cm}^{-1}$ . Furthermore, stretching vibration bands for C-OH bonds [26, 27] were observed at  $1386\text{ cm}^{-1}$  and for C-O bonds at  $1092\text{ cm}^{-1}$  [26-31]. The FT-IR spectra confirmed the presence of functional groups including hydroxyl (-OH), carbonyl (-C=O), and amino (N-H) groups on the surface of the synthesized CDs [32].

Hence, the sample was identified as belonging to the group of carbon nanodots (CNDs), specifically CQDs. These CQDs align with the expected characteristics, exhibiting nano-scale spherical morphology and distinctive carbon-based functional groups. The nano-sized particles and their aggregated structure, resulting from high surface energy and strong intermolecular interactions, are characteristic features of CQDs.

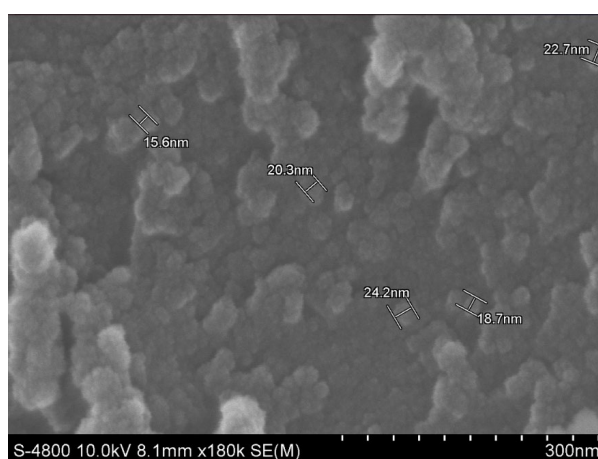


Figure 3. The SEM analysis results of the dried sample.

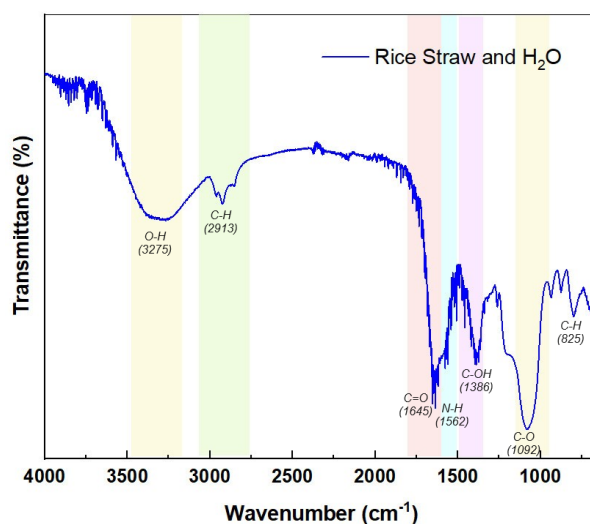


Figure 4. The FT-IR spectrum of CQDs derived from rice straw.

These findings indicated that the synthesized CQDs possess suitable properties for applications in wastewater filtration [29, 30], especially when combined with a technique that has the advantage of surface area/volume ratio, such as electrospinning [33, 34]. They exhibit the capability to adsorb various metal ions, including Hg, Fe, Cu, Cd, Pb, Zn, Cr, and fluoride [16, 30]. For instance, O-H and C-H groups have demonstrated potential for mercury adsorption from the environment, thereby contributing to mercury concentration reduction. Meanwhile, C=O and C-OH can form complexes with mercury, aiding in its absorption and retention in the environment. Moreover, in addition to their adsorption capabilities, carbon dots also exhibit fluorescence when exposed to fluoride and Fe ions [16, 17]. This dual functionality allows CQDs not only to purify water but also to serve as indicators of pollution levels in both water and air environments.

### 3.4. Optical properties of CQDs

Carbon quantum dots (CQDs) exhibit distinct optical absorption characteristics in the ultraviolet-visible (UV-Vis) spectrum. These absorption characteristics are fundamental to the photoluminescence behavior of CQDs, which often display excitation-dependent fluorescence—a property that can be leveraged in

various applications, including bioimaging, sensing, and optoelectronics. First, the optical properties of the obtained CQDs were determined using a Hitachi double-beam spectrophotometer (UV-Vis/NIR, FL) UH5300. For the sake of reproducibility, the parameters for the UV-Vis measurement are presented in Table 1. Then, the UV-Vis measurement results were presented in Figure 5.

The pronounced absorption peak at around 270 nm is attributed to the  $\pi$ - $\pi^*$  electronic transition of aromatic C=C bonds [1, 35]. This is a common feature of  $sp^2$  hybridized carbon domains within CQDs and suggests the presence of graphitic or graphene-like structures. This feature indicates the conjugated nature of the carbon framework in CQDs, which is critical for their optical properties and potential applications in bioimaging and optoelectronics. Next, the broad shoulder around 300–320 nm can be attributed to the  $n$ - $\pi^*$  transition involving nonbonding electrons from oxygen-containing functional groups such as hydroxyl (-OH), carboxyl (-COOH), or carbonyl (C=O) groups on the CQD surface [36]. Surface functional groups contribute to the photophysical properties and improve solubility, making CQDs suitable for aqueous-phase applications like biosensing. The lack of significant absorption beyond 400 nm suggested that these CQDs did not contain dopants (e.g., nitrogen,

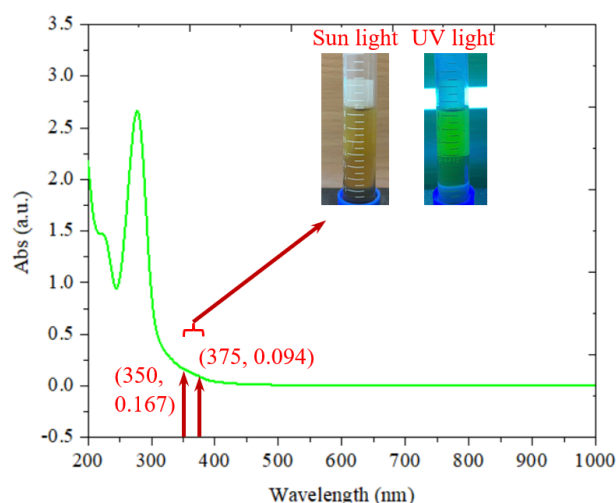


Figure 5. UV-Vis absorption spectrum of CQDs.

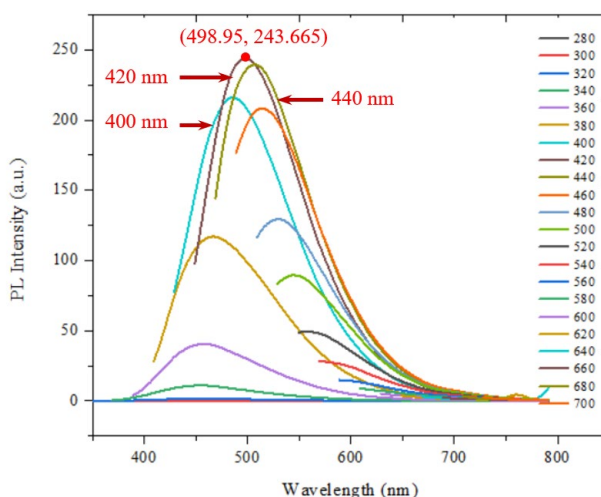


Figure 6. PL spectra of CQDs at different excitation wavelengths.

sulfur) or heteroatom modifications that could extend absorption into the visible region [37]. This indicated that their electronic structure was primarily carbon-based with minimal surface defects. This makes the CQDs less useful for visible light-driven applications but ideal for UV-blocking and UV-sensing technologies. From Figure 5, the high absorption intensity in the UV region signifies potential for UV photodetectors or UV shielding applications.

In the next step of optical properties research, a detailed photoluminescence (PL) study was performed using an Agilent Cary Eclipse fluorescence spectrophotometer with parameters as in Table 2. The provided PL spectrum of CQDs appeared to exhibit multiple excitation-dependent PL behaviors as shown in Figure 6.

In Figure 6, the emission peak shifted toward longer wavelengths (red-shift [36]) as the excitation wavelength increased from 280 nm to 700 nm. The intensity and position of the peaks varied significantly across the spectrum. This behavior was characteristic of CQDs and arises due to size distribution, surface-state emission, and heterogeneous structures [7, 36, 37]. CQDs of varying sizes were emitted at different wavelengths due to quantum confinement effects [7]. In addition, the PL emission peaks were broad, with full width at half maximum (FWHM) extending over tens of nanometers. Broad PL peaks indicated that different particle sizes contributed to emissions over a range of wavelengths. Furthermore, overlapping emissions from core states ( $sp^2$  domains) and surface states broaden the spectra [37]. Also from Figure 6, the PL intensity was highest when excited at long-wave UV-A (e.g., 400 nm). This occurs because CQDs absorbed UV light more efficiently due to  $\pi-\pi^*$  transitions in aromatic C=C bonds [7]. In the current study, the emission peak moves from blue (400–450 nm) to green or yellow (500–600 nm) as excitation increases. At longer excitation wavelengths, surface states dominated the emission [37]. The PL spectrum revealed key optical properties of the CQDs, including excitation-dependent emission, a broad emission band, and red shift. These characteristics reflected its potential in bioimaging, sensing, and optoelectronic applications [38]. The observations aligned with standard features of CQDs, where surface states and quantum confinement effects dominated their photophysical behavior.

Hence, the UV-Vis spectrum indicated suitable optical properties for pollutant interaction, while the PL spectrum confirmed strong fluorescence with excitation-dependent behavior, making these CQDs excellent candidates for sensing applications. For wastewater treatment (photocatalysis), further modifications, such as doping with elements like nitrogen or coupling with other semiconductors (e.g.,  $TiO_2$ , ZnO), are required to enhance visible-light absorption and reduce charge carrier recombination [39].

The particle size reported in our study is based on SEM analysis, which measures dried samples and may show larger sizes due to aggregation effects. Since SEM primarily provides surface morphology, it may not accurately represent the true size distribution of individual particles in solutions.

In this study, the analysis recognized that DLS, HR-TEM, or AFM could provide more precise measurements of the actual particle size in solution. However, based on our Fourier-transform Infrared Spectroscopy (FTIR) and Photoluminescence (PL) spectra, the synthesized materials exhibit optical characteristics and typical functional groups of CQDs, supporting their classification as CDs. To further improve accuracy, future studies could incorporate HR-TEM or DLS to confirm the size distribution of the particles in solution.

This study primarily focused on the synthesis, structural characterization, and optical properties (UV-Vis and PL spectra) of CQDs derived from rice straw, with an emphasis on their potential applications in wastewater filtration. While quantum yield (QY) is an important parameter, its measurement was not included in this work due to the absence of suitable standard reference material and the necessary instrumentation during our experimental phase. As QY provides valuable insight into the fluorescence efficiency of CQDs, particularly for applications in bioimaging, sensing, and optoelectronics. In future studies, comparative QY measurements using standard fluorophores are planned to be conducted as references to better assess the optical performance of the synthesized CQDs.

#### 4. Conclusions

The study focused on a method for preparing CQDs from rice straw. A bottom-up approach using a Teflon-covered hydrothermal reactor was utilized to synthesize CQDs. The obtained CQDs aqueous solutions showed a color change from yellow-brown to green, indicating the formation of CQDs. Furthermore, using this method, the CQDs achieved a size of approximately 20 nm. Additionally, functional groups such as O-H, C-H, C=O, N-H, C-OH, and C-O with different peak amplitudes were revealed by the FTIR testing method. Based on SEM imaging, which reveals nano-sized particles displaying agglomeration, and FTIR spectra indicating prominent peaks attributed to O-H, C=O, and C-OH bonds. The UV-Vis spectrum revealed optical properties well-suited for pollutant interaction, while the PL spectrum demonstrated strong fluorescence with excitation-dependent behavior, highlighting the potential of these CQDs as outstanding candidates for sensing applications. Hence, these findings indicated that the synthesized CQDs possess suitable properties for applications in wastewater filtration. Also, combining CQDs with fibrous nanomaterials capable of absorbing water and woven into a mesh represents a promising approach for wastewater sensing or water and air filtration applications.

#### Conflict of Interest

The authors declare that they have no conflict of interest.

#### References

1. Gayen B, Palchoudhury S, Chowdhury J. Carbon Dots: A Mystic Star in the World of Nanoscience. *J Nanomater.* 2019;2019:3451307. <https://doi.org/10.1155/2019/3451307>

2. Liu J, Li R, Yang B. Carbon Dots: A New Type of Carbon-Based Nanomaterial with Wide Applications. *ACS Cent Sci.* 2020;6:2118-27. <https://doi.org/10.1021/acscentsci.0c01306>
3. Behi M, Gholami L, Naficy S, Palomba S, Dehghani F. Carbon Dots: a novel platform for biomedical applications. *Nanoscale Adv.* 2022;4:353-76. <https://doi.org/10.1039/D1NA00559F>
4. Elugoke SE, Uwaya GE, Quadri TW, Ebenso EE. Carbon Quantum Dots: Basics, Properties, and Fundamentals. In: Berdimurodov E, Verma DK, Guo L, editors. *Carbon Dots: Recent Developments and Future Perspectives*. Washington, DC: American Chemical Society; 2024. p. 3-42. <https://doi.org/10.1021/bk-2024-1465.ch001>
5. Derya O, Mohammad AK, Rosalie KH, Bronwyn F. Properties, synthesis, and applications of carbon dots: A review. *Carbon Trends.* 2023;12:100276. <https://doi.org/10.1016/j.cartre.2023.100276>
6. Ye H-G, Lu X, Cheng R, Gou J, Li H, Wang C-F, et al. Mild bottom-up synthesis of Carbon Dots with temperature-dependent fluorescence. *J Lumin.* 2021;238:118311. <https://doi.org/10.1016/j.jlumin.2021.118311>
7. Nasrollahzadeh M, Sajjadi M, Sajadi SM, Issaabadi Z. Chapter 5: Green Nanotechnology. In: Nasrollahzadeh M, Sajadi SM, Sajjadi M, Issaabadi Z, Atarod M, editors. *Interface Science and Technology*. Amsterdam: Elsevier; 2019. p. 145-98. <https://doi.org/10.1016/B978-0-12-813586-0.00005-5>
8. Bhattacharya T, Do HA, Rhim J-W, Shin GH, Kim JT. Facile Synthesis of Multifunctional Carbon Dots from Spent Gromwell Roots and Their Application as Coating Agents. *Foods.* 2023;12:2165. <https://doi.org/10.3390/foods12112165>
9. Cheng C, Shi Y, Li M, Xing M, Wu Q. Carbon quantum dots from carbonized walnut shells: Structural evolution, fluorescence characteristics, and intracellular bioimaging. *Mater Sci Eng C Mater Biol Appl.* 2017;79:473-80. <https://doi.org/10.1016/j.msec.2017.05.094>
10. Sarkar S, Banerjee D, Ghorai UK, Chattopadhyay KK. Hydrothermal synthesis of carbon quantum dots and study of its photoluminescence property. In: 2016 International Conference on Microelectronics, Computing and Communications (MicroCom). Durgapur, India: IEEE; 2016. <https://doi.org/10.1109/MicroCom.2016.7522521>
11. Shen T, Wang Q, Guo Z, Kuang J, Cao W. Hydrothermal synthesis of carbon quantum dots using different precursors and their combination with TiO<sub>2</sub> for enhanced photocatalytic activity. *Ceram Int.* 2018;44:11828-34. <https://doi.org/10.1016/j.ceramint.2018.03.271>
12. Quang NK, Hieu NN, Bao VVQ, Phuoc VT, Ngoc LX, Doc LQ, et al. Hydrothermal synthesis of carbon nanodots from waste wine cork and their use in biocompatible fluorescence imaging. *New Carbon Mater.* 2022;37:595-602. [https://doi.org/10.1016/S1872-5805\(22\)60608-5](https://doi.org/10.1016/S1872-5805(22)60608-5)
13. Han Z, He L, Pan S, Liu H, Hu X. Hydrothermal synthesis of carbon dots and their application for detection of chlorogenic acid. *Luminescence.* 2020;35:989-97. <https://doi.org/10.1002/bio.3803>
14. Liu S, Liu Z, Li Q, Xia H, Yang W, Wang R, et al. Facile synthesis of carbon dots from wheat straw for colorimetric and fluorescent detection of fluoride and cellular imaging. *Spectrochim Acta A Mol Biomol Spectrosc.* 2021;246:118964. <https://doi.org/10.1016/j.saa.2020.118964>
15. Jorn-am T, Praneeraj J, Attajak R, Sirisit N, Manyam J, Paoprasert P. Quasi-solid, bio-renewable supercapacitor with high specific capacitance and energy density based on rice electrolytes and rice straw-derived carbon dots as novel electrolyte additives. *Colloids Surf A Physicochem Eng Asp.* 2021;628:127239. <https://doi.org/10.1016/j.colsurfa.2021.127239>
16. Al-Qahtani SD, Hameed A, Snari RM, Shah R, Alfi AA, Shaaban F, et al. Development of fluorescent carbon dots ink from rice straw waste toward security authentication. *J Mol Liq.* 2022;354:118927. <https://doi.org/10.1016/j.molliq.2022.118927>
17. Atchudan R, Edison TNJI, Chakradhar D, Perumal S, Shim J-J, Lee YR. Facile green synthesis of nitrogen-doped carbon dots using *Chionanthus retusus* fruit extract and investigation of their suitability for metal ion sensing and biological applications. *Sens Actuators B Chem.* 2017;246:497-509. <https://doi.org/10.1016/j.snb.2017.02.119>
18. Alabadi A, Razzaque S, Yang Y, Chen S, Tan B. Highly porous activated carbon materials from carbonized biomass with high CO<sub>2</sub> capturing capacity. *Chem Eng J.* 2015;281:606-12. <https://doi.org/10.1016/j.cej.2015.06.032>
19. Fathy NA, Basta AH, Lotfy VF. Novel trends for synthesis of carbon nanostructures from agricultural wastes. In: Abd-El salam KA, editor. *Carbon Nanomaterials for Agri-Food and Environmental Applications*. Amsterdam: Elsevier; 2020. p. 59-74. <https://doi.org/10.1016/B978-0-12-819786-8.00004-9>
20. Basta AH, Lotfy VF. Sustainable development of pulping by-product for limiting its pollution risk and production new aerogel-based carbon nanostructures for dyes adsorption. *J Clean Prod.* 2023;428:139275. <https://doi.org/10.1016/j.jclepro.2023.139275>
21. Bao Z, Lotfy VF, Zhou X, Fu S, Basta AH. Assessment of porous carbon from rice straw residues with potassium ferrate-assisted activation as cationic and anionic dye adsorbents. *Ind Crops Prod.* 2024;212:118298. <https://doi.org/10.1016/j.indcrop.2024.118298>
22. Lotfy VF, Basta AH. Enhancing the valorization of pulping black liquors in production effective aerogel-carbon nanostructure as adsorbents toward cationic and ionic dyes. *Sci Rep.* 2024;14:15236. <https://doi.org/10.1038/s41598-024-65136-8>
23. Yang J, Fu L, Wu F, Chen X, Wu C, Wang Q. Recent Developments in Activated Carbon Catalysts Based on Pore Size Regulation in the Application of Catalytic Ozonation. *Catalysts.* 2022;12:1085. <https://doi.org/10.3390/catal12101085>
24. Sohrabnezhad S, Rezaei Ochbelgh D, Morsali Golboos N. Irradiation with Neutrons and Formation of Simple Radiation Defects in Semiconductors. *Int J Nanosci Nanotechnol.* 2013;9:61-70.
25. Ahmadi P, Alamolhoda S, Mirkazemi SM. Phase Formation, Microstructure and Magnetic Properties of BiFeO<sub>3</sub> Synthesized by Sol-Gel Auto Combustion Method Using Different Solvents. *Int J Nanosci Nanotechnol.* 2017;13:195-201.
26. Aditya K, Avinash C, Pradeep B, Mohan KH, Venkataramaniah K, Indira KH. Comparative performance evaluation of carbon dot-based paper immunoassay on Whatman filter paper and nitrocellulose paper in the detection of HIV infection. *Microfluid Nanofluid.* 2016;20:1-13. <https://doi.org/10.1007/s10404-016-1763-9>
27. Marfa E, Aleksandra T, Svetlana AS. Optical Properties of Carbon Dots Synthesized by the Hydrothermal Method. *Materials (Basel).* 2023;16:4018. <https://doi.org/10.3390/ma16114018>
28. Taishu Y, Yoshiki I, Tetsuhiko I. Particulate, Structural, and Optical Properties of D-Glucose-Derived Carbon Dots Synthesized by Microwave-Assisted Hydrothermal Treatment. *ECS J Solid State Sci Technol.* 2017;7:R3034. <https://doi.org/10.1149/2.0091801jss>
29. Devi P, Rajput P, Thakur A, Kim K-H, Kumar P. Recent advances in carbon quantum dot-based sensing of heavy metals in water. *Trends Anal Chem.* 2019;114:171-95. <https://doi.org/10.1016/j.trac.2019.03.003>
30. Rani UA, Ng LY, Ng CY, Mahmoudi E. A review of carbon quantum dots and their applications in wastewater treatment. *Adv Colloid Interface Sci.* 2020;278:102124. <https://doi.org/10.1016/j.cis.2020.102124>
31. Qutub N, Sabir S. Optical, Thermal and Structural Properties of CdS Quantum Dots Synthesized by A Simple Chemical Route. *Int J Nanosci Nanotechnol.* 2012;8:111-20.
32. Sajjad K, Mina H, Mojtaba A-M. Co-phthalocyanine/Graphene Quantum Dots/TiO<sub>2</sub> as a New Hybrid for Photocatalytic

- Degradation of Formic Acid Toward Hydrogen Generation. *Int J Nanosci Nanotechnol.* 2024;20:25-32. <https://doi.org/10.22034/ijnn.2024.548254.2162>
33. Jang J-W, Min K-E, Kim C, Shin J, Lee J, Yi S. Review: Scaffold Characteristics, Fabrication Methods, and Biomaterials for the Bone Tissue Engineering. *Int J Precis Eng Manuf.* 2023;24:511-29. <https://doi.org/10.1007/s12541-022-00755-7>
34. Nguyen TK, Nguyen VT. Study of an Electrospinning Process Using Orthogonal Array. *Int J Precis Eng Manuf.* 2024;25:2153-61. <https://doi.org/10.1007/s12541-024-01049-w>
35. Norman A, Mohd Jaaffar AK, Jamaludin NS, Shirotsaki Y, Saad N, Che Abdullah CA. Cocoa Pod Husks as Precursors for Biosynthesis of Carbon Dots as Potential Bioimaging Tool. *Int J Nanosci Nanotechnol.* 2022;18:79-92.
36. Jamaludin N, Tan TL, Zaman ASK, Sadrolhosseini AR, Rashid SA. Acid-Free Hydrothermal-Extraction and Molecular Structure of Carbon Quantum Dots Derived from Empty Fruit Bunch Biochar. *Materials (Basel).* 2020;13:3356. <https://doi.org/10.3390/ma13153356>
37. Li H, Kang Z, Liu Y, Lee S-T. Carbon nanodots: synthesis, properties, and applications. *J Mater Chem.* 2012;22:24230-53. <https://doi.org/10.1039/c2jm34690g>
38. Valarmathy C, Sudhakarimala S. Carbon Dots as Selective Fluorescent Probes for Metal Ions-Influence of *Moringa oleifera* Leaf as a Precursor. *Int J Nanosci Nanotechnol.* 2023;19:263-75. <https://doi.org/10.22034/ijnn.2023.2006835.2398>
39. Kwee Y, Kristanti AN, Sharon M, Fahmi MZ. A Review of Promising Selected Agents Combined with Carbon Dots for Biomedical Applications. *Int J Nanosci Nanotechnol.* 2022;18:11-44.